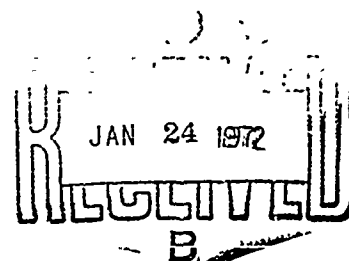# School of Engineering

AIR FORCE INSTITUTE OF TECHNOLOGY

Air University

ON THE ATTENUATION OF DIVERGING SHOCK WAVES

IN A POROUS MATERIAL

Peter J. Torvik

AFIT TR 71-4

November 1971

JAN 24 1972

RECEIVED

B

Wright-Patterson Air Force Base, Ohio

49

DOCUMENT CONTROL DATA - R & D

(Security classificat on of title, body of abstract and indexing annotation must be entered wnen the overall report is classified)

1. ORIGINATING ACTIVITY (Corporate author)	2a. REPORT SECURITY CLASSIFICATION
Air Force Institute of Technology (AFIT-EN) Wright-Patterson AFB, Ohio 45433	Unclassified
	2b. GROUP

3. REPORT TITLE

On the Attenuation of Diverging Shock Waves in a Porous Material

4. DESCRIPTIVE NOTES (Type of report and inclusive dates)

AFIT Technical Report

5. AUTHOR(S) (First name, middle initial, last name)

Peter J. Torvik

6. REPORT DATE	7a. TOTAL NO OF PAGES	7b. NO OF REFS
November 1971	41	3

8a. CONTRACT OR GRANT NO	9a. ORIGINATOR'S REPORT NUMBER(S)
b. PROJECT NO.	AFIT TR 71-4
c.	9b. OTHER REPORT NO(S) (Any other numbers that may be assigned this report)
d.	

10. DISTRIBUTION STATEMENT

Approved for public release, distribution unlimited.

11. Approved for release; IAW AFR 190-17 *Keith A. Williams* KEITH A. WILLIAMS, 2nd Lt., USAF Assistant Director of Information, AFIT	12. SPONSORING MILITARY ACTIVITY

13. ABSTRACT

Several approximate theories for predicting the attenuation rate of shockwaves in porous materials are developed. The material is assumed to be an ideal locking solid. Cylindrical and Spherical geometries are considered, with the shockwave assumed to be generated by several different mechanisms, including the instantaneous deposition of momentum and the rapid deposition of energy over the interior of a cavity in the porous material. The generation of shockwaves through the adiabatic expansion of a cavity filled with an ideal gas at high pressure is also considered with a model based on conservation of momentum and a model based on conservation of energy. The predictions of six simple models are compared for the case of a cylindrical wave in a material having low porosity, including a model which is analagous to the familiar "snowplow" model.

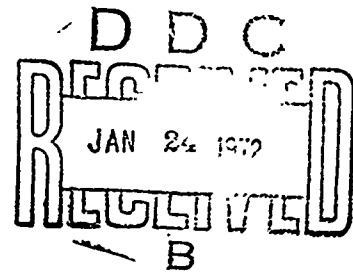| 14. KEY WORDS	LINK A		LINK B		LINK C	
	ROLE	WT	ROLE	WT	ROLE	WT
Shock attenuation						
Porous media						
Snowplow model						

ON THE ATTENUATION OF DIVERGING SHOCK WAVES

IN A POROUS MATERIAL

Peter J. Torvik

Associate Professor of Mechanics

Air Force Institute of Technology

Technical Report - AFIT TR 71-4

November 1971

DDC

JAN 24 1972

B

School of Engineering
Air Force Institute of Technology
Wright-Patterson Air Force Base, Ohio

Figures

Figures

iii

Symbols

$d\phi$ — Incremental angle enclosing material segment

$D(R)$ — Propagation speed at time shock has propagated a distance R.

E_K, E_I — Total kinetic and internal energies behind the shock front

e_K, e_I — Kinetic energy per unit mass, internal energy

H — Total momentum in material segment

I_O — Applied impulse per unit area

P_O — Initial pressure of gas in cavity

P — Pressure immediately behind the disturbance front

R — Radius of shock front at time t

R_O — Initial cavity radius

R — Radius of cavity during expansion

r — Radial coordinate

s — Dimensionless cavity radius, R/R_O

t — time

U_O, U — Displacement of cavity boundary and general particle

x — Dimensionless shock radius, R/R_O

v_r — Radial particle velocity behind front

$V(R)$ — Radial particle velocity at shock front

W — Work done by the expansion of perfect gas within the cavity

α — Ratio of initial to final specific volume

β — Compressibility parameter, $1 - \rho_O/\rho_f$

γ — Ratio of specific heats for perfect gas

ε_O — Total energy deposited on cavity wall, per unit area

κ — Parameter describing energy deposition rate

iv

Symbols (Cont.)

ρ_O — Density of porous material before compaction

ρ_f — Density of porous material after compaction

τ, ξ — Dummy Variables

I. Introduction

An underground explosion generates a strong shock wave which propagates through the earth, but the strength of this shock wave diminishes with distance for a number of reasons. In the case of a cylindrical (line) source, or a spherical (point) source, geometric attenuation, i.e., the distribution of the original energy (or momentum) over larger material volumes as the disturbance progresses necessarily leads to lower shock pressures at later times. In this work, several models of this process are proposed and investigated. Waves diverging in both cylindrical and spherical coordinates are considered. Models based on the assumption of an instantaneous deposition of a known energy (or momentum) on the interior of a cavity are developed, as well as models based upon a continuous transfer of energy (or momentum) from the material within the cavity to the surrounding medium through the mechanism of cavity expansion.

It was the goal of this investigation to develop several simple models, no one of which is expected to be most appropriate for all applications. In any given situation, the appropriate model is best determined through a comparison of the various predictions with that available data which most closely matches the conditions of interest.

The simple models to be presented each satisfy only conservation of energy or conservation of momentum, rather than both, as the true solution must. Consequently, none of these models should be regarded as exact solutions to any physical problem. In all cases, the material

1

through which the shock propagates is assumed to be an ideal locking material. The limitations of this assumption have been discussed elsewhere [1].

This report is organized as follows. In Section II, models based on conservation of momentum are developed. First, a "snowplow" model for an impulse instantaneously applied over the interior of a spherical cavity is given. This is followed by a model for the gradual transfer of momentum to the surrounding material by the expansion of a spherical cavity initially filled with gas at high pressure. Finally, both of these cases are considered for the geometry of a cylindrical wave. In Section III several models based on conservation of energy are discussed. First, a model for the rapid deposition of energy over the interior of a spherical cavity is given. Next, a model for the gradual transfer of energy from the contents of a spherical cavity to the surrounding medium is developed. This is followed by the analogous results for these two cases in the cylindrical geometry, and finally models based on a simplifying assumption about the spatial energy distribution are considered. The report terminates with a comparison of the predictions of various models for a specific case and a short summary.

2

II. Momentum Models

While it is recognized that the total momentum in a symmetrically diverging cylindrical or spherical wave is zero, in the absence of shear stresses momentum within any infinitesimal solid angle should also be conserved. The following models are developed in that spirit. An extension of the "snowplow" model (as discussed in Ref [1]) to spherical coordinates is first considered.

a. Prescribed Impulse, Spherical Coordinates

We wish to determine the rate of decay of the pressure pulse which results when a prescribed impulse per unit area is applied to the interior surface of a spherical cavity of radius R_o. We assume that the material containing the cavity is initially of density ρ_o, but that the application of a pressure pulse compacts the material to a final density, ρ_f, which is independent of the applied pressure.

We consider a region of the material, as shown in Figure 1a, where the radius R is the location of the disturbance front at some time after the application of the pressure pulse. R_o and R are values of the Lagrangian radius coordinate identifying the region of interest. It is convenient to employ the radius R as the time-like variable in recording the progress of the event. During the time required for the disturbance to travel the distance to R, the inner radius has moved a distance U_c which is a function of time, or alternatively, a function of the current disturbance radius, R. At any time the location of the inner boundary, in the Eulerian description, is as shown in Figure 1b, or

3
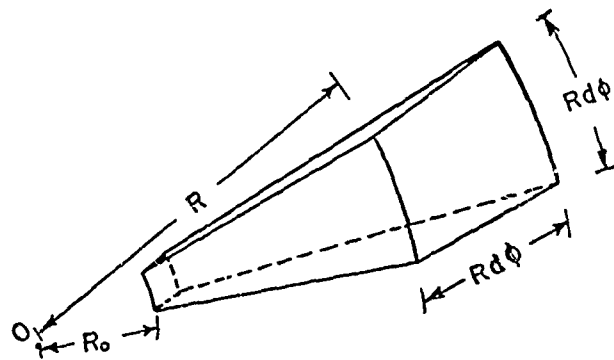
a. REGION OF INTEREST
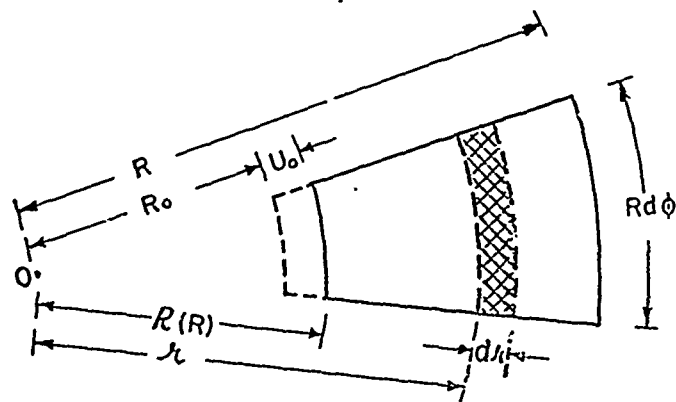
b. KINEMATICS OF CAVITY EXPANSION

Figure 1 Geometry of Deformation

4

$$R(R) = R_O + U_O(R) \qquad (1)$$

We assume the spherically symmetric velocity field has only a radial component, V_r, and denote by $V(R)$ the particle velocity immediately behind the disturbance front. In terms of an Eulerian radius, the radial velocity field must be divergence free if the continuity equation is to be satisfied, as the assumption of an ideal locking solid leads to a uniform density behind the disturbance front. Thus

$$v_r = V(R) \frac{R^2}{r^2} \qquad (2)$$

The displacement at the inner cavity radius is

$$U_O = \int_{t=0}^{t(R)} V(R) \frac{R^2}{R(R)^2} \, dt \qquad (3)$$

where $t(R)$ denotes the time required for the disturbance to reach R. Denoting by $D(R)$ the rate of propagation of the disturbance, i.e.,

$$D(R) = \frac{dR}{dt}$$

we may write Equation 3 as

$$U_O = \int_{R_O}^{R} \frac{V(R)}{D(R)} \frac{R^2}{[R(R)]^2} \, dR \qquad (4)$$

Substitution into Equation 1 yields an integral equation for R as a function of R which may be solved if $V(R)$ and $D(R)$ are known.

At the disturbance front, the Rankine-Hugoniot jump relationships must be satisfied in order to insure the conservation of mass and momentum across the disturbance. Thus

$$\rho_O D(R) = \rho_f [D(R) - V(R)] \qquad (5)$$

$$P(R) = \rho_O D(R) \, V(R) \qquad (6)$$

5

where $P(R)$ is the pressure immediately behind the front measured with respect to the initial pressure. From the first of these, it is seen that the ratio of velocities in Equation 5 remains constant for an ideal locking material, and

$$\frac{V(R)}{D(R)} = 1 - \rho_o|\rho_f = \beta \tag{8}$$

Equation 1 then becomes

$$R(R) = R_o + \beta \int_{R_o}^{R} \frac{R^2}{R(R)^2} \, dR \tag{9}$$

which has the solution

$$R(R) = \left[\beta R^3 + (1 - \beta)R_o^3\right]^{1/3} \tag{10}$$

This relationship may be more easily obtained by equating the mass contained in a hollow sphere of density ρ_o and radii R and R_o with that contained in a hollow sphere of density ρ_f and radii R and R.

The mass and momentum contained in a length dr of the region of interest are, from Figure 1b,

$$dm = \rho_f (rd\phi)^2 dr \tag{11}$$

$$dh = \rho_f v_r(r) r^2 dr (d\phi)^2 \tag{12}$$

At the time when the disturbance has reached R, the total momentum behind the disturbance is

$$H = \int_{R(R)}^{R} \rho_f v_r(r) r^2 dr (d\phi)^2 \tag{13}$$

If an impulse, I_o, per unit initial area is supplied at $t = 0$ over the inner cavity $R = R_o$, we have from the balance of impulse and momentum,

$$H = I_o R_o^2 (d\phi)^2 \tag{14}$$

6

Substituting expression for the velocity field (Equation 2) into Equation 13, we find that

$$H = \rho_f V(R) \; R^2 \; [R - \mathcal{R}(R)] \, (d\phi)^2 \tag{15}$$

where $\mathcal{R}(R)$ is as given in Equation 10.

Combining Equations 7 and 8 so as to eliminate the disturbance speed yields

$$P(R) = \rho_o \frac{V(R)^2}{\beta} \tag{16}$$

The expression for the attenuation of the peak pressure as a function of distance is found by substituting Equations 14 and 15 into Equation 16, or

$$P(R) = \frac{I_o^2 \; R_o^4}{\rho_o \; R^4 \; [R - \mathcal{R}(R)]^2} \cdot \frac{(1 - \beta)^2}{\beta} \tag{17}$$

At large values of R/R_o, the inner radius $\mathcal{R}$ can be seen, from Equation 10, to asymptotically approach

$$\mathcal{R}(R) = \beta^{1/3} \; R \tag{18}$$

Hence, at large R,

$$P(R) = \frac{I_o^2 \; R_o^4}{\rho_o \; R^6} \; \frac{(1 - \beta)^2}{\beta(1 - \beta^{1/3})^2} \tag{19}$$

i.e., the pressure decays as the sixth power of distance.

For values of R only slightly greater than R_o, we may set $R = R_o + \epsilon$, where $\epsilon \ll R_o$. Then, from Equation 10,

$$\mathcal{R}(R) \cong R_o + \beta\epsilon \tag{20}$$

and the decay of pressure with the distance becomes, for small ϵ,

$$P(x) = \frac{I_o^2}{\rho_o \beta \epsilon^2} \tag{21}$$

7

When written in terms of a ratio of specific volumes, α, customarily defined through

$$\alpha = \frac{v_O}{v_{SO}} = \frac{\rho_f}{\rho_O} = (1 - \beta)^{-1} \qquad (22)$$

Equation 21 becomes the familiar result of the one dimensional, or "snow-plow" theory [1], for the attenuation of a plane wave,

$$P = \frac{I_0^2 \, \alpha^2 \, v_{SO}}{\epsilon^2 (\alpha - 1)} \qquad (23)$$

where v_{SO} is the specific volume of the fully compacted solid.

Equation 17 can be put into a form useful for comparing the attenuation as a function of porosity through substituting Equation 8 into Equation 17, or

$$\hat{P} = P(R) \, \frac{R_O^2 \, \rho_f}{I_O^2} = \frac{(1-\beta)}{\beta} \, \frac{R_O^6}{R^4 (R - R)^2} \qquad (24)$$

The decay of the dimensionless pressure $\hat{P}$ is given as a function of the dimensionless distance in Figure 2. Results for several values of β are given. For purposes of comparison, a line with slope of -6 is also shown. For values of $R/R_O > 3$ the pressure decays essentially as the sixth power of the distance, as is predicted by Equation 19. It can also be seen that the predicted rate of decay appears to be slower for $\beta = 0.9$ (high porosity) than for $\beta = 0.1$ (low porosity), but it should be noted that the weight of material required to produce a given pressure reduction will be substantially less for the material of higher porosity.

In Figure 3, the dimensionless pressure is given as a function of the distance, $R/R_O - 1$, measured from the edge of the cavity. For small distances, the decay is seen to be as the inverse square of the
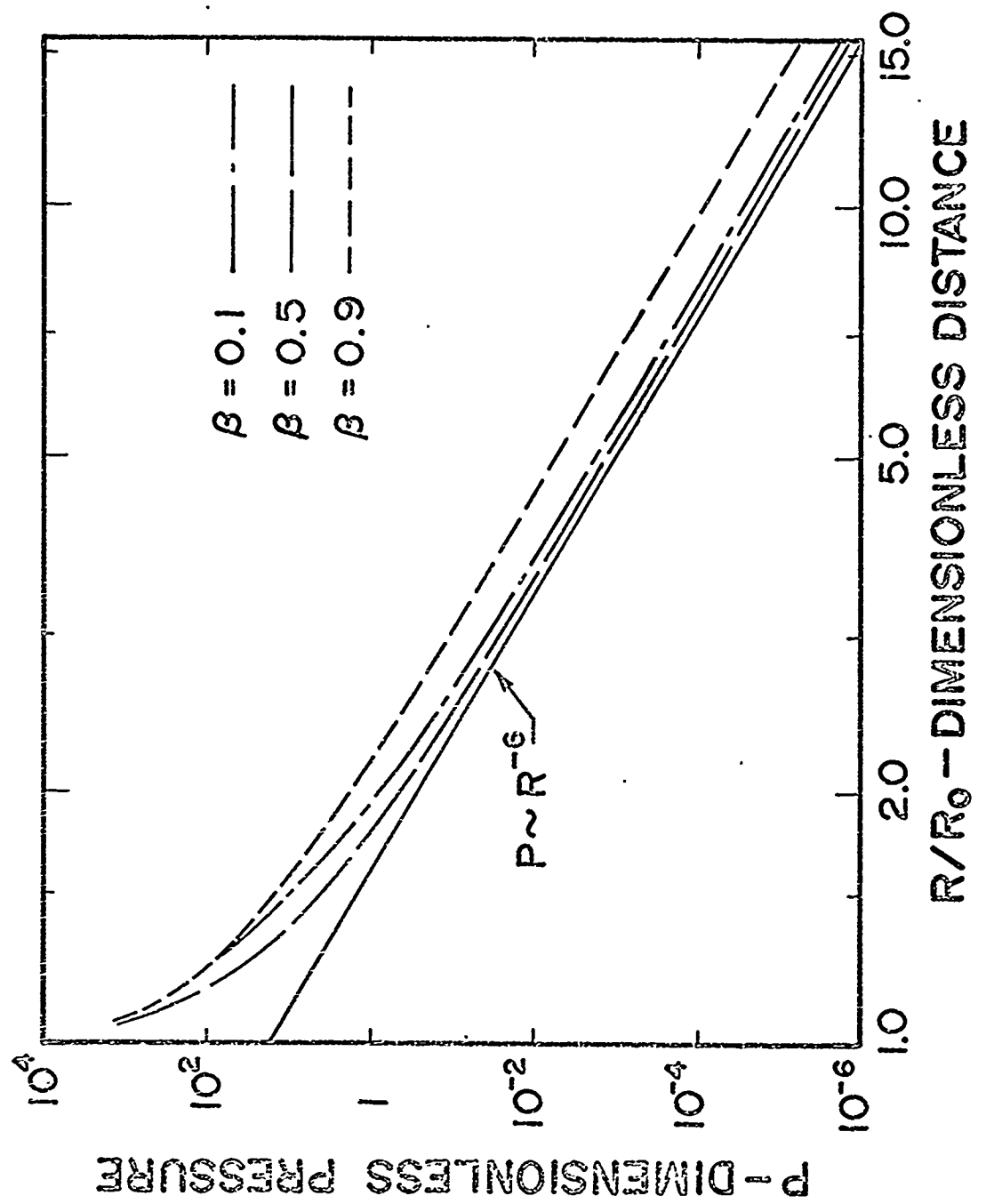
8

Figure 2 Pressure Decay with Distance for the Spherical "Snowplow" Model
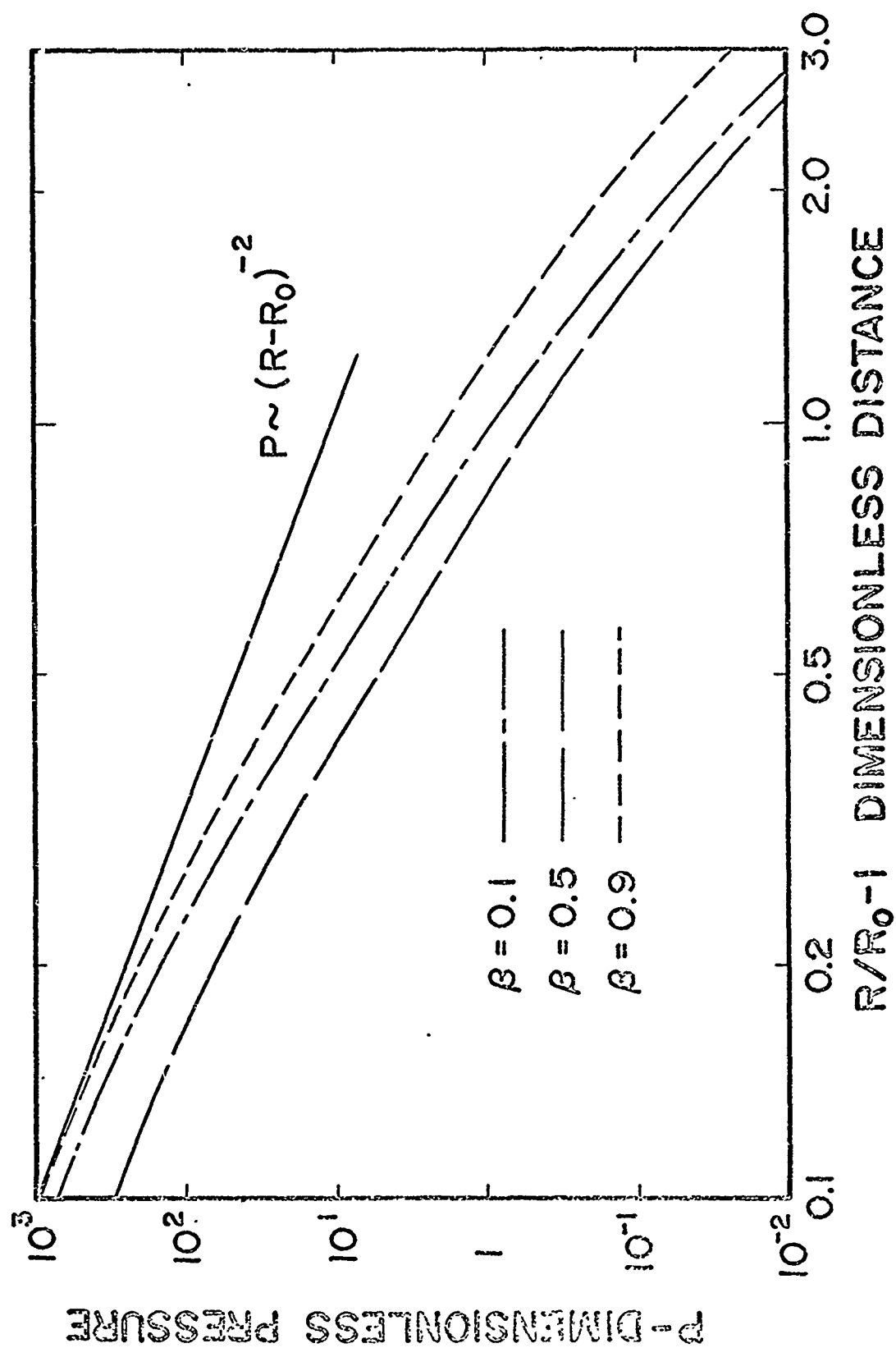
Figure 3   Pressure Decay Near Spherical Source, "Snowplow" Model

distance, in accord with Equation 23, and as the inverse sixth power for large distances.

Since the velocity field is known (Equation 2), the pressure distribution behind the shock front can also be determined. From local conservation of momentum,

$$\rho_f \left[\frac{\partial v_r}{\partial t} + v_r \frac{\partial v_r}{\partial r} \right] = - \frac{\partial P}{\partial r} \tag{25}$$

with the pressure at $r = R$ given by Equation 17 and the velocity field given by Equation 2. The time derivative in Equation 25 can be re-written as

$$\frac{\partial v_r}{\partial t} = \frac{\partial v_r}{\partial R} \frac{dR}{dt} = D\left[\frac{\partial V(R)}{\partial R} \frac{R^2}{r^2} + \frac{2V(R)R}{r^2} \right] \tag{26}$$

where the shock speed D is also a function of the current shock radius R and the particle velocity at the shock front is given by Equation 15. Substituting into Equation 25 and integrating, we find that the pressure distribution is given by

$$\frac{P(r)}{P(R)} = 1 - \frac{\beta}{1 - \beta} \left[\frac{1}{\beta} \frac{R}{R - R} \left\{ 1 - \beta \frac{R^2}{R^2} \right\} (\frac{R}{r} - 1) + \frac{1}{2} (\frac{R^4}{r^4} - 1) \right] \tag{27}$$

In Figures 4a, 4b, and 4c, the pressure distribution behind the front is given at several instants of time (shock radius) for several values of porosity. The substantial growth, with time, of the inner radius of the cavity, R, is evident. Examination of these pressure profiles reveals negative pressures in the region near the inner cavity radius. These tensions result from the "hoop" strains becoming so large as to produce a net increase in volume (dilatation) which, for the assumed isotropic state of stress, results in a radial stress which
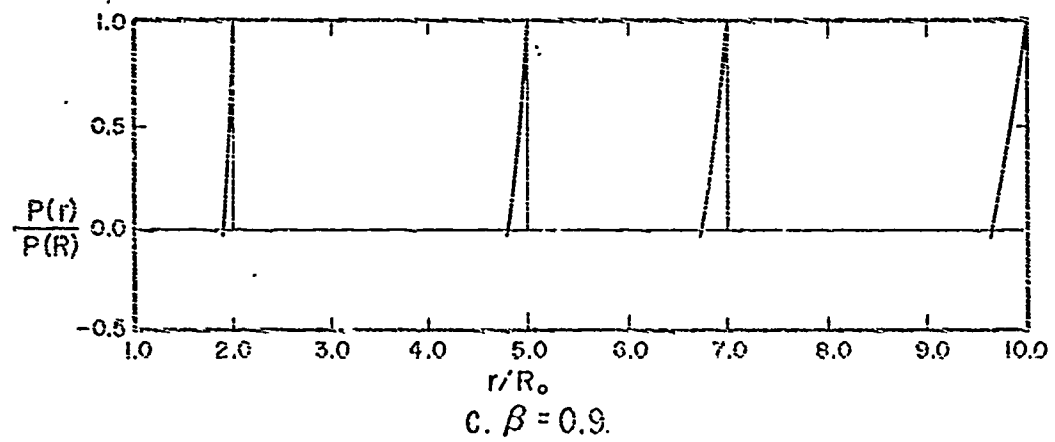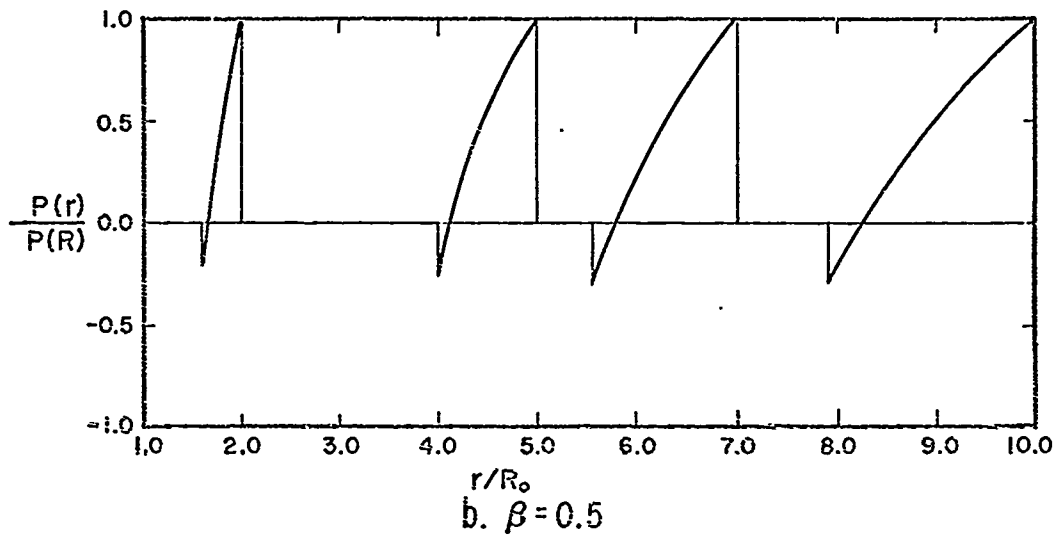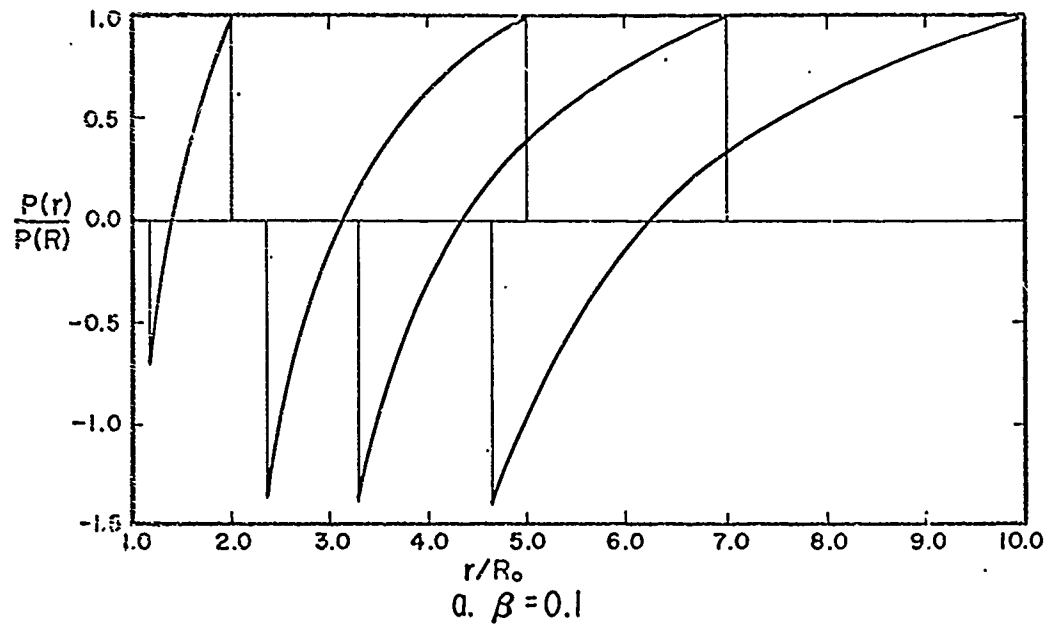
11

Figure 4   Pressure Distribution Behind Shock for Various Porosities

is positive. For highly porous materials, however, this tensile stress is small compared to the peak stresses, and it may be assumed that the solution has reasonable validity for predicting the pressures at the shock front in spite of the physical unreality of the tension near the inner cavity.

b. Expansion of a Spherical Cavity

In the preceeding section, the decay of the pressure pulse resulting from the instantaneous application of a prescribed impulse over the interior surface of a spherical cavity was considered. In this section, the decay of the pressure wave generated by the application of a prescribed pressure will be treated. This problem has been considered previously and some asymptotic results obtained [2].

The expression given (Equation 13) for the total momentum behind the expanding spherical front is valid independent of the means by which the shock wave is generated as is the kinematical relationship (Equation 10) relating the current location of the inner cavity radius to the current shock radius. Hence, if a pressure $P(t)$ is applied commencing at time zero, the total impulse delivered can be written as

$$I(t) = \int_0^t P(\tau) R(\tau)^2 (d\phi)^2 d\tau \tag{28}$$

and equated to the total momentum at that instant, as given in Equation 13. We assume here that the pressure supplied is sufficient to keep the material fully compacted.

Of particular interest is the case where the cavity is filled with a gas at high pressure which expands and drives a spherical shock into the porous material. We will assume a perfect gas at initial

13

pressure P_O. Thus

$$P(R) R^{3\gamma} = P_O R_O^{3\gamma} \qquad (29)$$

where γ is the ratio of specific heats, assumed to be constant. Again using the current shock radius, R, as the time-like variable, the total impulse, Equation 28, may be rewritten and equated to the total momentum. From 15 and 8, we then have

$$\beta \int_{R_O}^{R} P_O \frac{R_O^{3\gamma}}{R^{3\gamma}} R^2 \frac{d\xi}{V} = \frac{H}{(d\phi)^2} = \rho_f V(R) R^2 [R - R] \qquad (30)$$

A differential equation may be obtained through differentiating with respect to R. This yields

$$\beta P_O \frac{s^{(2-3\gamma)}}{\rho_f} = V(x) \frac{d}{dx} \left\{ V(x) \ x^2 [x - s(x)] \right\} \qquad (31)$$

where

$$x = R/R_O$$
$$s = R/R_O = [\beta x^3 + 1 - \beta]^{1/3}$$

After rewriting as

$$\frac{d}{dx} [\frac{1}{2} v^2 p^2] = P_O \beta \ s^{(2-3\gamma)} p/\rho_f \qquad (32)$$

where $p = x^2(x-s)$, the shock front pressure may be written as

$$\frac{P(x)}{P_O} - 1 = \frac{2(1-\beta)}{x^4 (x-s)^2} [I_1 + I_2] = \frac{2(1-\beta)}{x^4 (x-s)^2} \int_1^{R/R_O} s^{(2-3\gamma)} \xi^2 (\xi - s) d\xi \qquad (33)$$

where

$$I_1 = \int_1^{R/R_O} \xi^3 [\beta \xi^3 + 1 - \beta]^{(2-3\gamma)/3} d\xi \qquad (34)$$

and

$$I_2 = - \int_1^{R/R_O} \xi^2 [\beta \xi^3 + 1 - \beta]^{(1-\gamma)} d\xi \qquad (35)$$

14

The second these is readily integrated through the substitution

$$y = \beta x^3 + 1 - \beta \tag{36}$$

to yield

$$I_2 = \frac{-1}{3\beta(2-\gamma)} \left[\left\{ \beta x^3 + 1 - \beta \right\}^{2-\gamma} - 1 \right] \tag{37}$$

The first integral is not as readily evaluated. For the case of $\gamma = 5/3$, however, the transformation given by Equation 36 yields

$$I_1 = \frac{1}{3\beta^{4/3}} \int_{1}^{\beta x^3 + 1 - \beta} \frac{[y-1+\beta]^{1/3}}{y} \, dy \tag{38}$$

which may be evaluated through the use of the following integral [3]

$$\int \frac{3\sqrt{u}}{y} \, dy = 3\sqrt[3]{u} + a \left\{ \frac{1}{a^{2/3}} \left[\frac{3}{2} \ln\left(\frac{3\sqrt{u} - 3\sqrt{a}}{3\sqrt{y}} \right) \right. \right. \tag{39}$$

$$\left. \left. - \sqrt{3} \tan^{-1}\left(\frac{\sqrt{3} \; \sqrt[3]{u}}{3\sqrt{u} + 2 \sqrt[3]{a}} \right) \right] \right\}$$

where $u = a + by$

For γ other than 5/3, Equation 34 can be integrated numerically without difficulty.

The decay of pressure, with distance, of the peak shock pressure is given in Figure 5 for $\gamma = 5/3$ and several values of β. It can be seen that the rate of decay increases with distance, varying from approximately $P/P_o \sim (R/R_o)^{-3}$ for small R/R_o to approximately $P/P_o \sim (R/R_o)^{-5}$ for large R/R_o.

In Figure 6, the decay of pressure with distance in a medium of $\beta = 0.5$ is compared for various values of γ. At large R, the asymptotic behavior is an $P \sim R^{-3\gamma}$, as can be readily deduced from Equation 33. This is in agreement with the results of Ref [2]. The result for $\gamma = 0$ corresponds to a constant pressure,
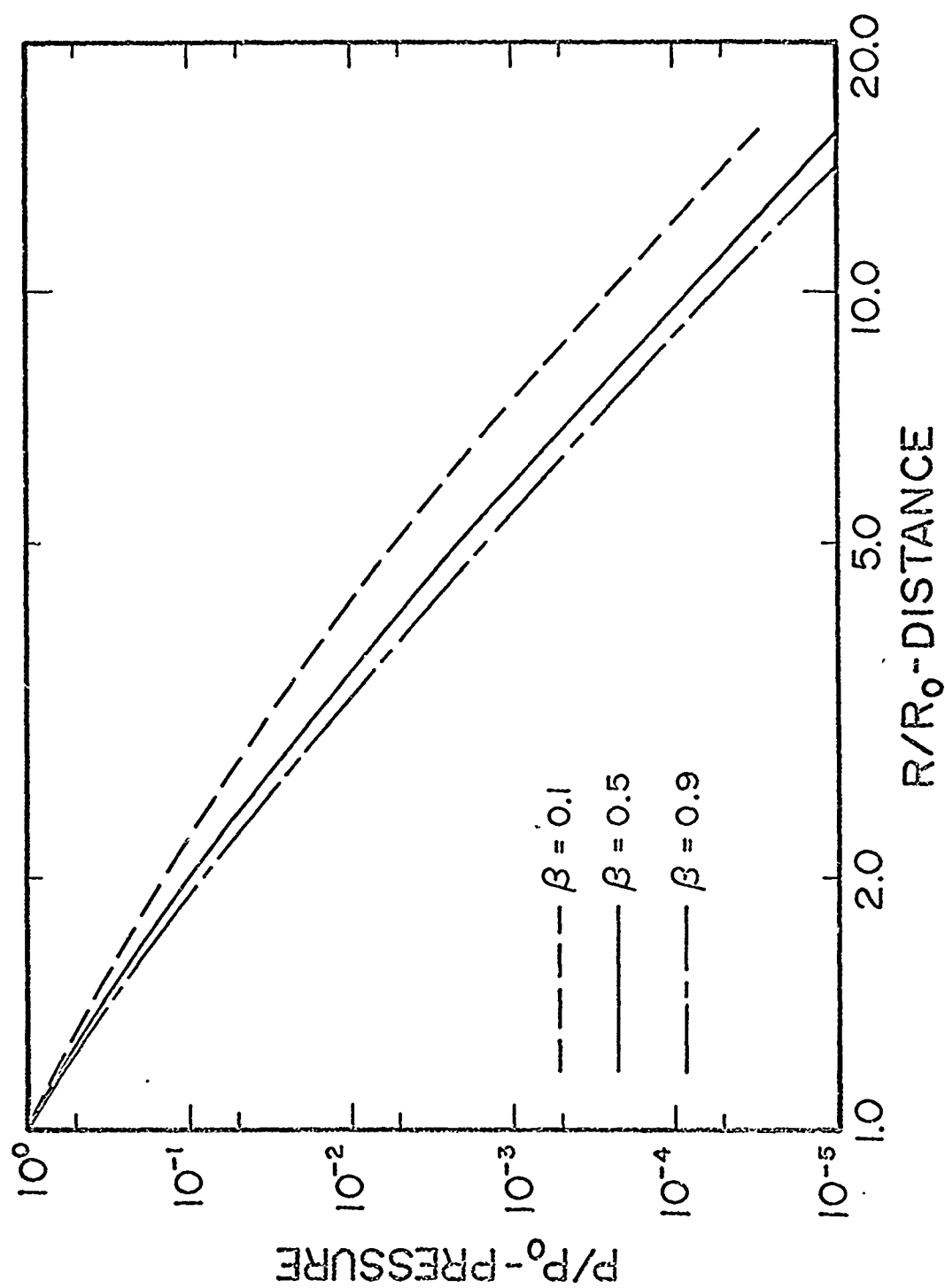
15

Figure 5   Decay of Shockwave Resulting from Expansion of Spherical
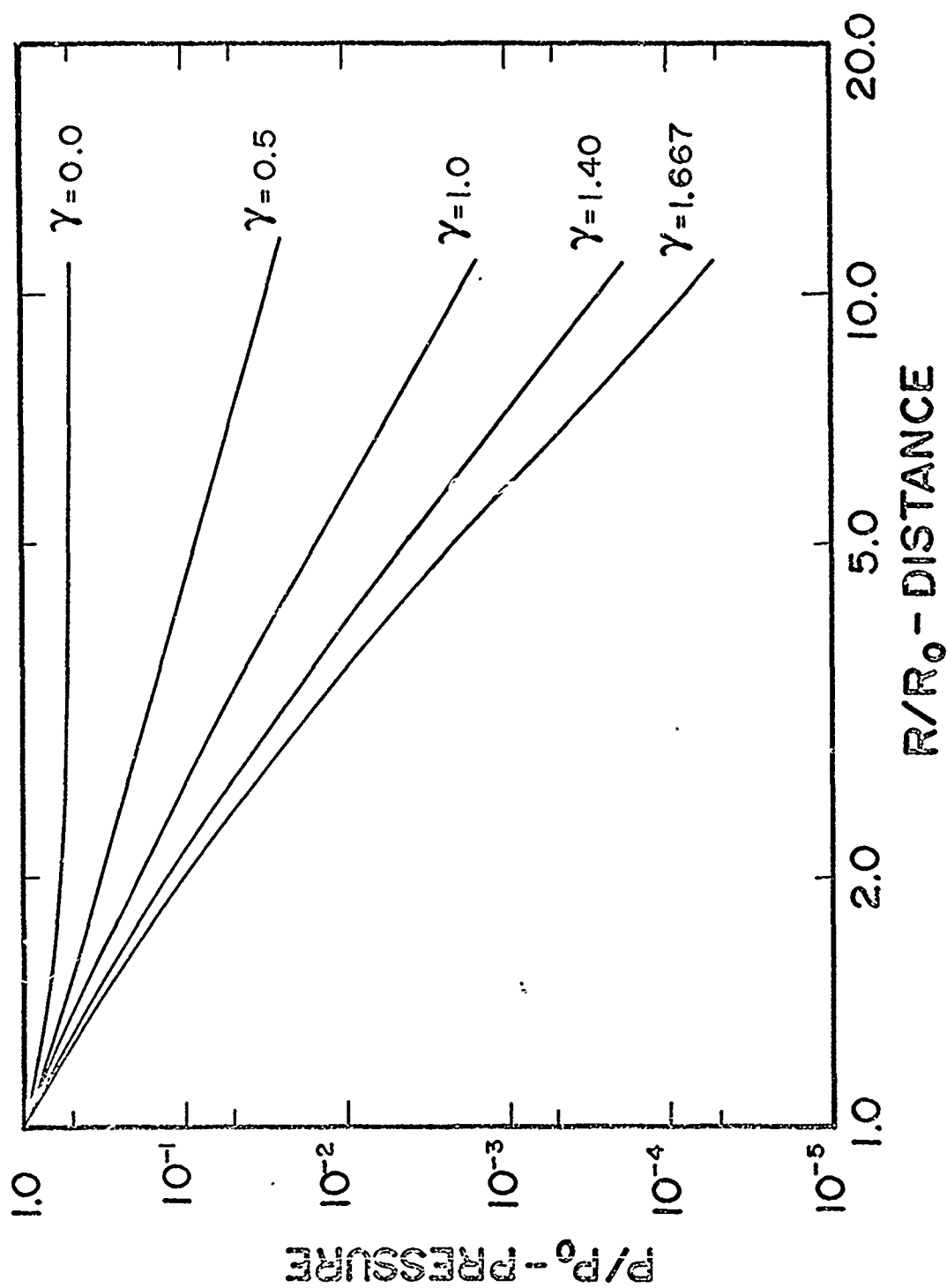Cavity, Momentum Model with $\gamma = 5/3$, for Materials of Various
Porosities

16

Figure 6 Decay of Spherical Shock Wave in Porous Material, $\beta = .5$, Resulting from Expansion of Various Gasses. Momentum Model

17

$\gamma = 1.0$ corresponds to an isothermal expansion, and $\gamma = 1.4$ and
$\gamma = 1.667$ correspond to the adiabatic expansion of air and a monotonic
gas, assumed to be ideal. $\gamma = .5$ has no physical interest, but is
included for purposes of comparison. These results were obtained by
the numerical integration of Equation 33 using step sizes of $\Delta R/R_o = $
0.001 for $1.01 \le R/R_o \le 1.1$, $\Delta R/R_o = 0.01$ for $1.1 \le R/R_o \le 2$ and
$\Delta R/R_o = 0.1$ for $2 \le R/R_o \le 11$. Pressures at the extreme points of
these ranges were found to agree typically to three or four significant
digits whether obtained with 10 or 100 integration steps. The results
obtained numerically for the case of $\beta = 0.5$ and $\gamma = 5/3$ as given in
Figure 6 show excellent agreement with the results for the same case
obtained through evaluation of the closed form expression and given in
Figure 5.

c. Momentum Models for Cylindrical Waves

The analyses given in the previous sections are readily modified
to be applicable to an expanding cylindrical wave, as might be generated
by the detonation of a line charge of high explosive imbedded in a
porous material.

In cylindrical coordinates the appropriate divergence free velocity
field is

$$v_r = V(R) \, \frac{R}{r} \tag{40}$$

The relationship between the inner cavity radius and the shock front
radius which must be satisfied in order to insure global conservation
of mass is

$$\rho_o \pi \, dz[R^2 - R_o^2] = \rho_f \pi \, dz[R^2 - R^2] \tag{41}$$

18

or

$$R = [\beta R^2 + (1 - \beta) R_o^2]^{1/2} \tag{42}$$

which takes the place of Equation 10, previously developed for the spherical case.

The momentum contained in an element of angle $d\theta$, width dz and length dr is

$$dh = \rho_f \, dz \, rd\theta \, dr \, v_r \tag{43}$$

Thus, when the disturbance has reached a distance R, the total momentum in the segment is

$$H = \int_R^R \rho_f \, dz \, d\theta \, v_r \, rdr = \rho_f \, dz \, d\theta \, V(R) \, R(R - R) \tag{44}$$

If an impulse, I_o, per unit initial area is applied over the inner cavity radius at $t = 0$, the balance of impulse and momentum leads to

$$I_o R_o = \rho_f \, V(R) \, R \, (R - R) \tag{45}$$

The predicted rate of decay of the shock front pressure then follows from solving Equation 45 for $V(R)$ and substituting the result into Equation 16

$$P(R) = \frac{I_o^2 R_o^2}{\rho_o} \frac{(1 - \beta)^2}{\beta} \frac{1}{R^2(R - R)^2} \tag{46}$$

where R is as given in Equation 42. This result may be termed the "snowplow" model for the cylindrical wave. At large R, $R(R) \sim \sqrt{\beta} \, R$

$$P(R) = \frac{I_o^2 R_o^2}{\rho_o} \frac{(1 - \beta)^2}{\beta} \frac{1}{[1 - \sqrt{\beta'}]^2} \frac{1}{R^4} \tag{47}$$

Indicating that the pressure decays as the fourth power of distance, at large R.

19

As before, the pressure distribution behind the shock may be found by integrating the momentum equation. The result is

$$\frac{P(r)}{P(R)} = 1 - \frac{\beta}{1-\beta} \left[\frac{1}{\beta} \frac{R}{R-R} \left(1-\beta \frac{R}{R}\right) \ln \frac{R}{r} + \frac{1}{2} \left(\frac{R^2}{r^2} - 1\right) \right] \tag{48}$$

Negative pressures will again occur near the cavity. In particular, at large R, $R \sim \beta\sqrt{R}$ and the pressure on the surface of the cavity is predicted to be

$$\frac{P(R)}{P(R)} = 1 - \frac{1}{1-\beta} \left[\ln \frac{1}{\beta} + \frac{1}{2} (1-\beta) \right] \tag{49}$$

which is negative for any β.

The solution for the expansion of a cylindrical cavity filled with a perfect gas may also be obtained in a manner similar to that given previously for the spherical case.

The impulse generated by the expansion is

$$I = \int_0^t P(\tau) \Big|_{r=R} d\theta \, R(\tau) \, d\tau \, dz \tag{50}$$

Changing the variable of integration yields

$$I = \int_{R_0}^R P(R) \, d\theta \, dz \, R(\xi) \, \beta \frac{d\xi}{V(\xi)}$$

Equating this to the total momentum given by Equation 44 yields

$$\beta \int_{R_0}^R P(R) \, R(\xi) \frac{d\xi}{V(\xi)} = \rho_f \, V(R) \, R \, (R-R) \tag{52}$$

which is to be solved for the shock front particle velocity, as a function of distance. For the adiabatic expansion of a cylindrical cavity filled with a perfect gas,

$$P(R) = P_o \, (R_o/R)^{2\gamma} \tag{53}$$

20

Differentiating Equation 52 with respect to R, as before, and defining

$$x = R/R_o$$
$$s = \dot{R}/R = [\beta x^2 + 1 - \beta]^{1/2} \tag{54}$$
$$p = x(x - s)$$

Equation 52 may be written as

$$\frac{d}{dR} \left[\frac{V^2 p^2}{2} \right] = \frac{\beta P_o R_o^{2\gamma}}{\rho_f} \cdot p R^{1-2\gamma} \tag{55}$$

Replacing V^2 by the pressure, through the use of Equation 16, leads to an expression for the peak shock pressure as a function of shock radius

$$\frac{P(x)}{P_o} = \frac{2(1-\beta)}{x^2 (x-s)^2} \int_1^x s^{(1-2\gamma)} \xi(\xi - s) d\xi \tag{56}$$

Equation 56 bears a high degree of resemblance to the analagous expression previously given for the spherical wave (Equation 33), and was integrated numerically in the manner previously described. Results obtained by the numerical integration of Equation 56 are given in Figure 7 for the case of $\gamma = 5/3$ and various values of β, and in Figure 8 for $\beta = .5$ and several values of γ.
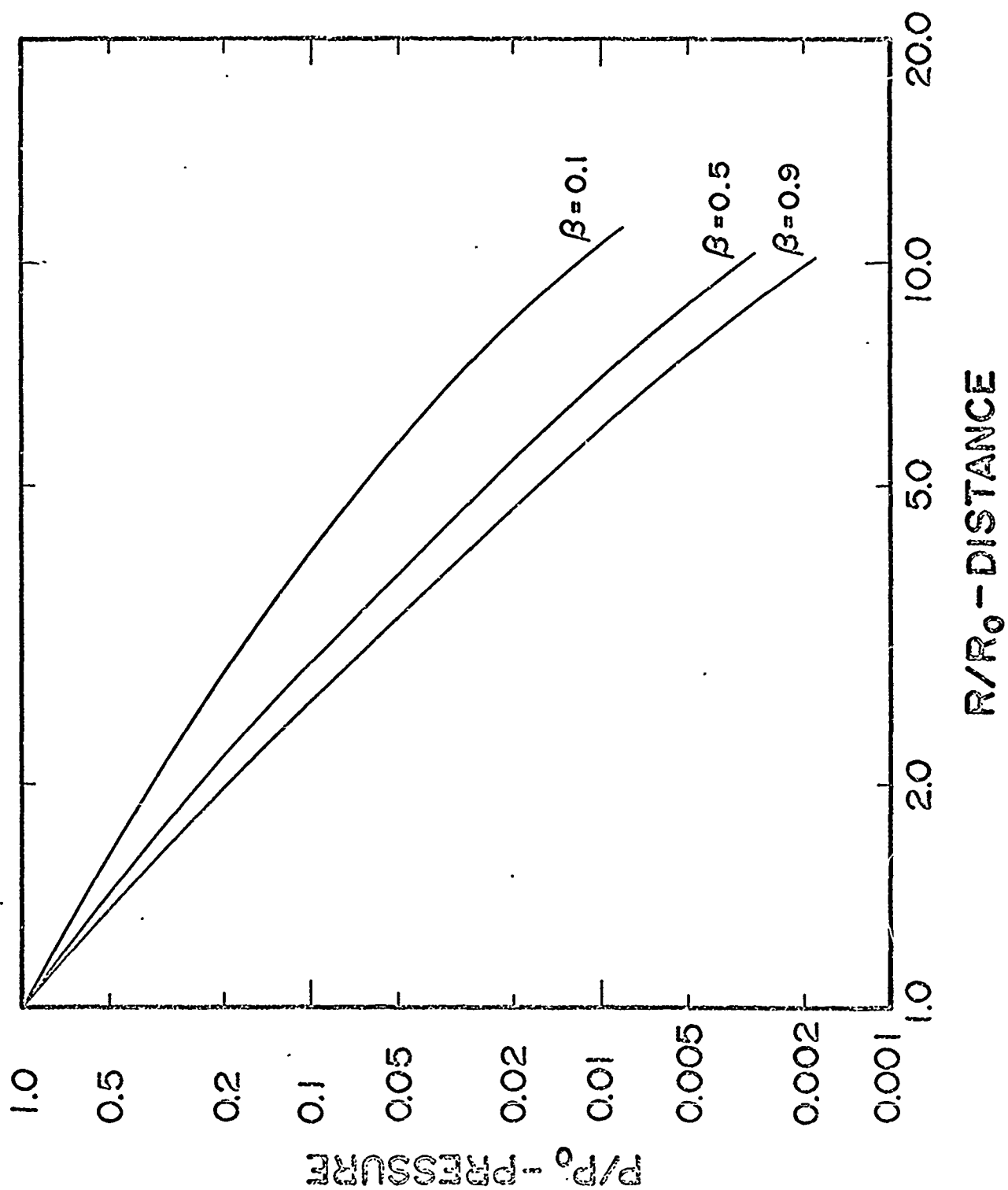
Figure 7   Decay of Cylindrical Shock Wave Resulting from Cavity

Expansion for Materials of Various Porosities. Momentum
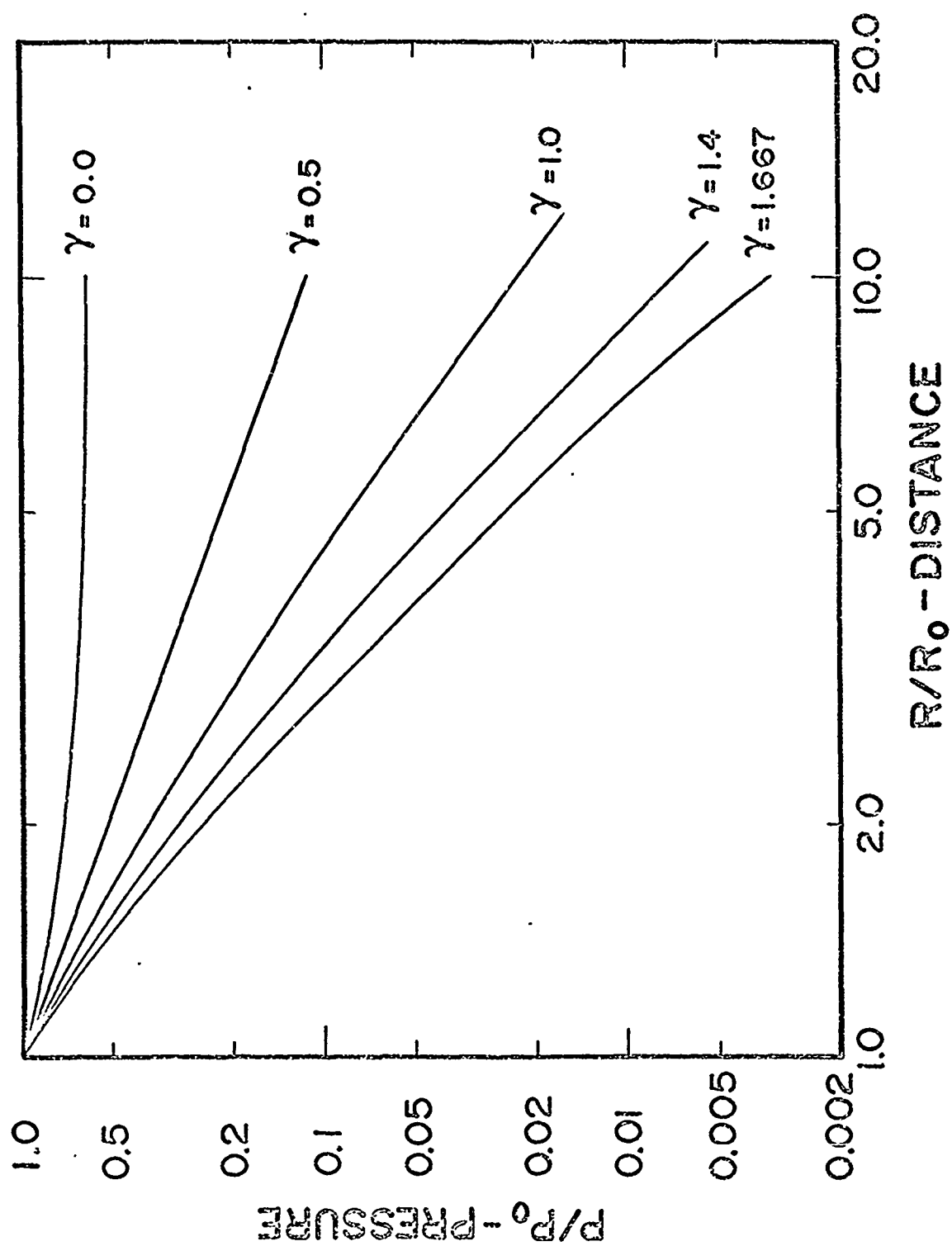
Model with $\gamma = 5/3$ 22

Figure 8 Decay of Cylindrical Shock Wave in Porous Material, $\beta = .5$,

Resulting from Expansion of Various Gasses. Momentum Model

III. Energy Models

The models given in the preceeding sections resulted from enforcing conservation of radial momentum. It is also possible to develop predictions of the pressure attenuation rate by considering the conservation of energy. The principal difficulty in this approach is the uncertainty as to the internal energy changes which can occur in a material of constant density.

a. Prescribed Deposition of Energy in Spherical Cavity

For a spherically diverging wave, the divergence free velocity field is

$$v_r = V(R) \frac{R^2}{r^2} \tag{57}$$

where $V(R)$ is the particle velocity immediately behind the shock front and is related to the shock speed by Equation 8. The kinetic energy between the shock front and the expanding cavity is

$$E_K = \int_R^R \frac{\rho f}{2} v_r^2 \, r^2 \, (d\phi)^2 dr \tag{58}$$

From Equations 16 and 8, this may be rewritten as

$$E_K = \frac{\beta P(R)}{2(1-\beta)} R^3 \left[\frac{R}{R} - 1 \right] (d\phi)^2 \tag{59}$$

where R is as given by Equation 10.

Immediately behind the shock front, the kinetic energy per unit mass is

$$e_K(R) = \frac{1}{2} V(R)^2 \tag{60}$$

and, from the Rankine-Hugoniot jump condition for energy, the increase in internal energy per unit mass is

24

$$e_I(R) = \frac{P}{2} \left\{ \frac{1}{\rho_O} - \frac{1}{\rho_f} \right\} \tag{61}$$

Substitution of Equations 16 and 8 into Equation 61 shows that

$$e_I(R) = e_K(R) = \frac{1}{2} V(R)^2 \tag{62}$$

i.e., that the internal and kinetic energies per unit mass are identical at the shock front.

For a material of the ideal locking nature under consideration, no volume changes can occur behind the shock front. Thus, if there are no reactions, losses due to viscosity, or any heat transfer, the energy of each particle must remain constant at the value acquired upon passage through the shock front. The particle initially at a distance r from the origin will therefore acquire and retain an increase in energy per unit mass of

$$e_I(r) = \frac{\beta}{2\rho_O} \left. P(r) \right|_{r=R} \tag{63}$$

The total internal energy is then easily computed in Lagrangian coordinates, and is found to be

$$E_I = \frac{\beta(d\phi)^2}{2} \int_{R_O}^{R} P(r) r^2 dr \tag{64}$$

If a known energy (per unit area) of ϵ_O is instantaneously deposited over the interior of a spherical cavity of radius R_O, an energy balance requires that

$$\epsilon_O R_O^2 (d\phi)^2 = E_K + E_I \tag{65}$$

throughout the entire process. Here E_K is given by Equation 59 and E_I is given by Equation 64. Satisfaction of this energy balance for all time (i.e., for all R) leads to a decay of peak shock pressure, with distance, which is the solution of the equation

25

$$\varepsilon_o R_o^2 = \frac{\beta P R^3}{2(1-\beta)} \left[\frac{R}{R} - 1 \right] + \frac{\beta}{2} \int_{R_o}^{R} P(\xi)\xi^2 d\xi \qquad (66)$$

This is a singular integral equation, the solution of which is singular at $R = R_o$ for the physical reason that a finite energy is being deposited into a zero volume. In any plausible physical process, this will not occur. Rather, the deposition of energy will require a finite time. An arbitrary deposition relationship

$$\varepsilon = \varepsilon_o \left[1 - \exp\{ - \kappa(R-R_o)/R_o \} \right] \qquad (67)$$

was selected. In this case, 90% of the energy is deposited in the time required for the shock to propagate $(\ell n 10)/\kappa$ cavity radii into the material. The resulting integral equation is

$$\varepsilon_o R_o^2 \left[1 - \exp\{ - \kappa(R-R_o)/R_o \} \right] = \frac{\beta}{2} \frac{P R^3}{(1-\beta)} \left[\frac{R}{R} - 1 \right] \qquad (68)$$
$$+ \frac{\beta}{2} \int_{R_o}^{R} P(\xi)\xi^2 d\xi$$

A solution to this equation was obtained by numerical integration, with results as given in Figure 9 for several arbitrarily selected values of κ and β. The instantaneous deposition of energy corresponds to $\kappa \to \infty$.

b. Expansion of a Spherical Cavity

Instead of assuming some arbitrary prescription of the deposition of energy, we may assume that the shock is generated by a prescribed pressure applied over the cavity boundary.

The work done on the surrounding material during such an expansion is

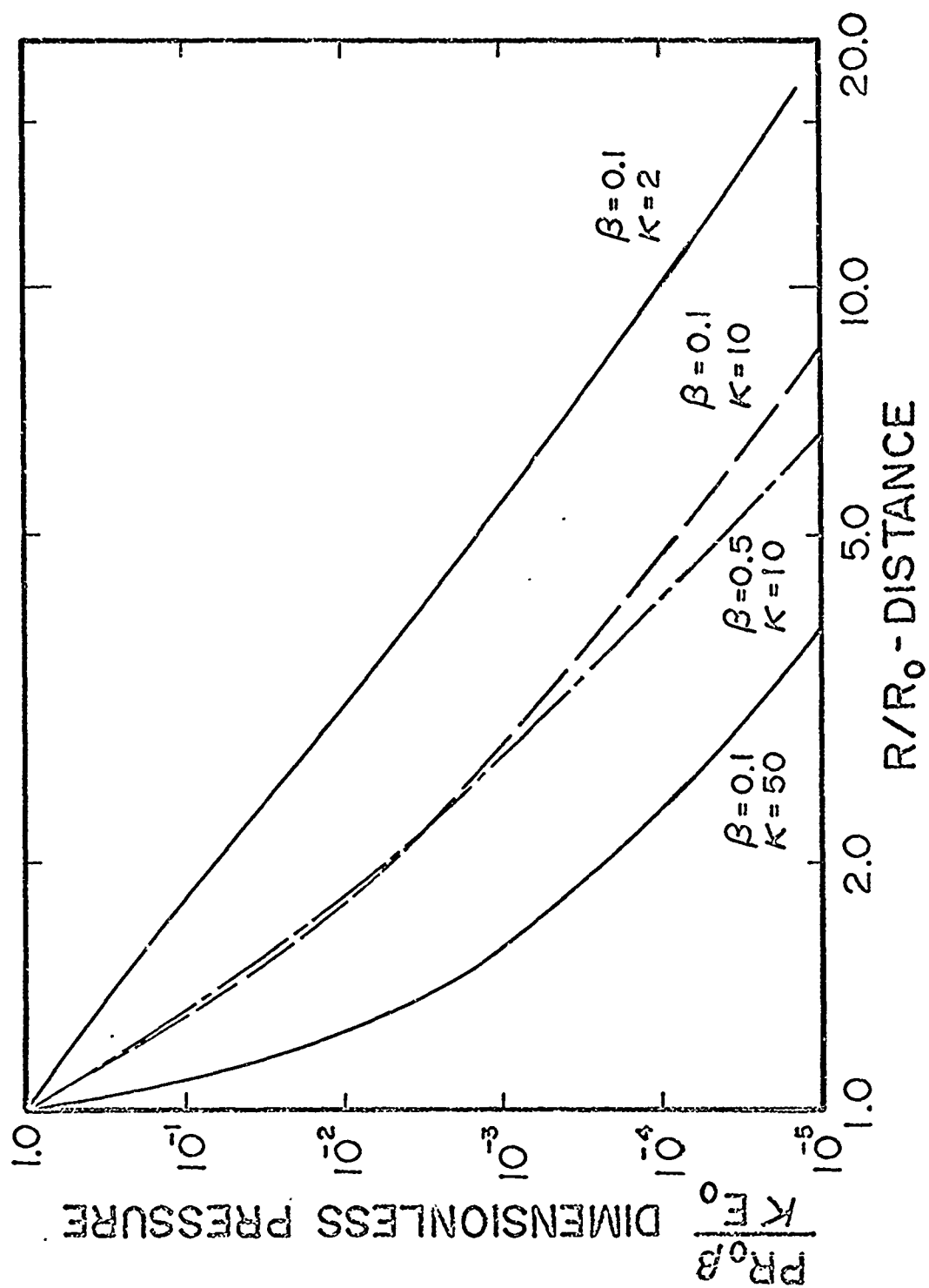$$W = \int_{R_o}^{R} P(\xi)\xi^2 (d\phi)^2 d\xi \qquad (69)$$

26

Figure 9 Attenuation of Spherical Shock Wave in Various Porous Materials – Shock Generated by Energy Deposition. Energy Model

27

where $P(\xi)$ is the pressure, a prescribed function of shock distance.
In particular, if the pressure results from the expansion of a spherical
cavity initially of radius R_o and filled with a perfect gas at initial
pressure P_o.

$$P(R)R^{3\gamma} = P_o R_o^{3\gamma}$$

or

$$W = \frac{P_o R_o^3 (d\phi)^2}{3(\gamma-1)} \left[1 - (R_o/R)^{3(\gamma-1)}\right] \tag{70}$$

Equating this work done to the kinetic and internal energies ac-
quired by the material through the passing of the shock leads to

$$W = E_K + E_I$$

where W is given by Equation 70, E_K by Equation 59 and E_I by Equation 64.
The resulting integral equation is

$$\frac{P_o R_o^3}{3(\gamma-1)} \left[1 - (\frac{R_o}{R})^{3(\gamma-1)}\right] = \frac{\beta P(R) R^3}{2(1-\beta)} \, (\frac{R}{R} - 1) + \frac{\beta}{2} \int_{R_o}^{R} P(\xi)\xi^2 d\xi \tag{71}$$

This equation (which is not singular) was solved numerically with
results as given in Figure 10.

c. Energy Models for Cylindrical Waves

For a cylindrically diverging wave, the divergence free velocity
field is

$$V_r = V(R) \frac{R}{r} \tag{72}$$

and the total energy behind the front is

$$E_K = \int_R^R \frac{\rho_f}{2} v^2(R) \frac{R^2}{r^2} \, rd\theta dz dr \tag{73}$$

or

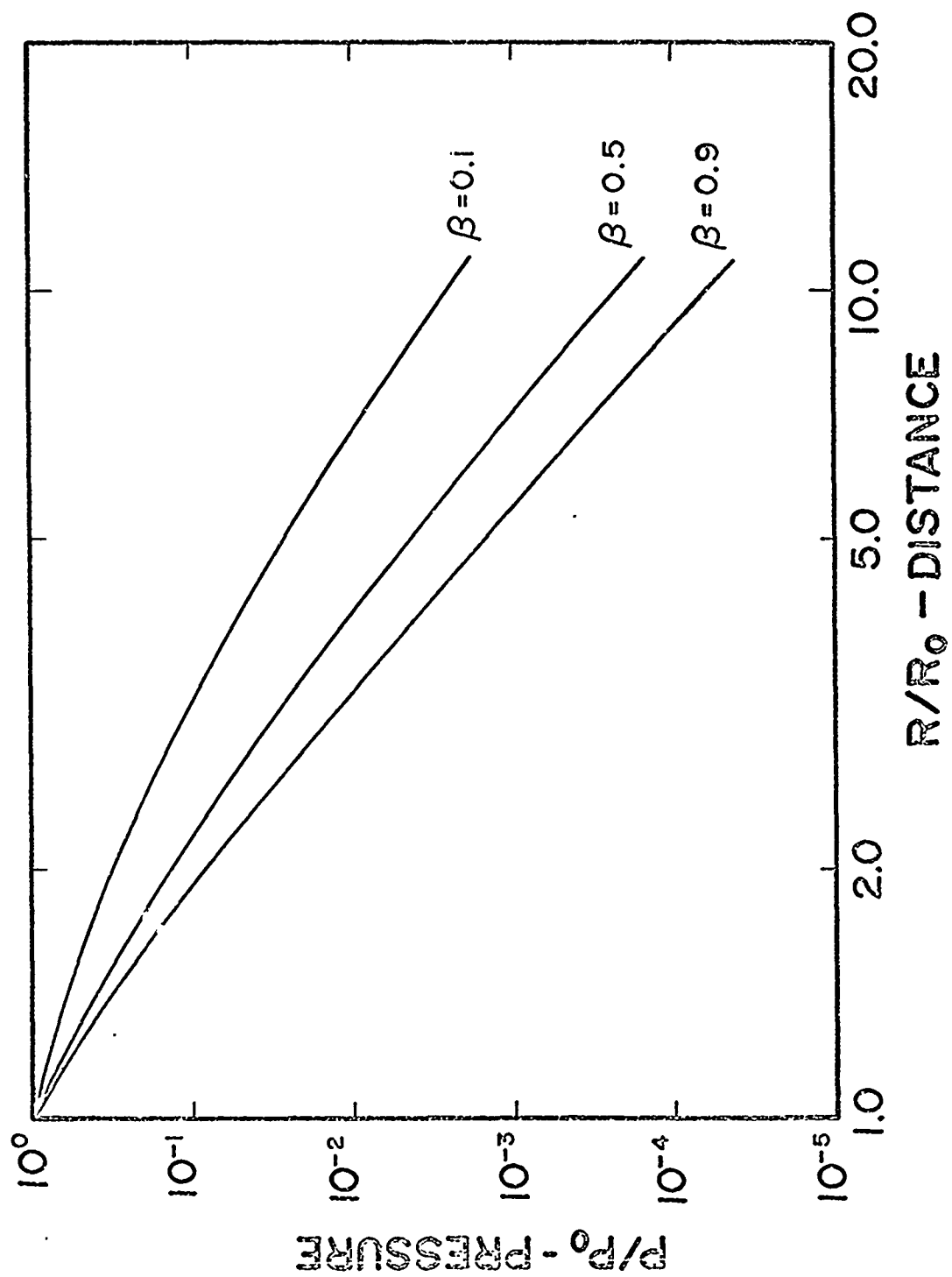$$E_K = \frac{\beta}{2(1-\beta)} P(R) \, R^2 \, \ln \frac{R}{R} \, d\theta dz \tag{74}$$

28

Figure 10 Attenuation of Spherical Shock Wave in Various Porous Materials –
Shock Generated by Cavity Expansion. Energy Model with $\gamma = 5/3$

29

R is again given by Equation 42. Assuming, as before, that the internal energy of each particle remains constant at the value acquired in passing through the front,

$$e(r) = \left. \frac{P(r)\beta}{2\rho_o} \right|_{r = R} \tag{75}$$

Thus

$$E_I = \int_{R_o}^{R} \rho_o e(\xi)\,\xi d\theta dz d\xi \tag{76}$$

$$= \frac{\beta}{2} \int_{R_o}^{R} P(\xi)\,\xi d\xi d\theta dz$$

For a deposition of total energy, ε_o, per unit area, over the interior of a cylindrical cavity, in accordance with Equation 67, the energy balance leads to a pressure distance relationship of which is the solution of

$$\varepsilon_o R_o \left[1 - \exp\left\{-\kappa(R-R_o)/R_o\right\}\right] = \frac{\beta}{2(1-\beta)}\, P(R)\, R^2 \ell n\left(\frac{R}{R}\right) + \frac{\beta}{2}\int_{R_o}^{R} P(\xi)\,\xi d\xi \tag{77}$$

The limiting case of an instantaneous deposition is obtained in the limit as $\kappa \to \infty$. A solution of this equation obtained by numerical integration is shown on Figure 11, for several values of κ and β.

For the case of the expanding cylinder, the work done is

$$W = \int_{R_o}^{R} P(R)\, R dR d\theta dz \tag{78}$$

For the expansion of a cylinder of radius R_o of perfect gas which expands adiabatically,

$$P(R) R^{2\gamma} = P_o R_o^{2\gamma} \tag{79}$$
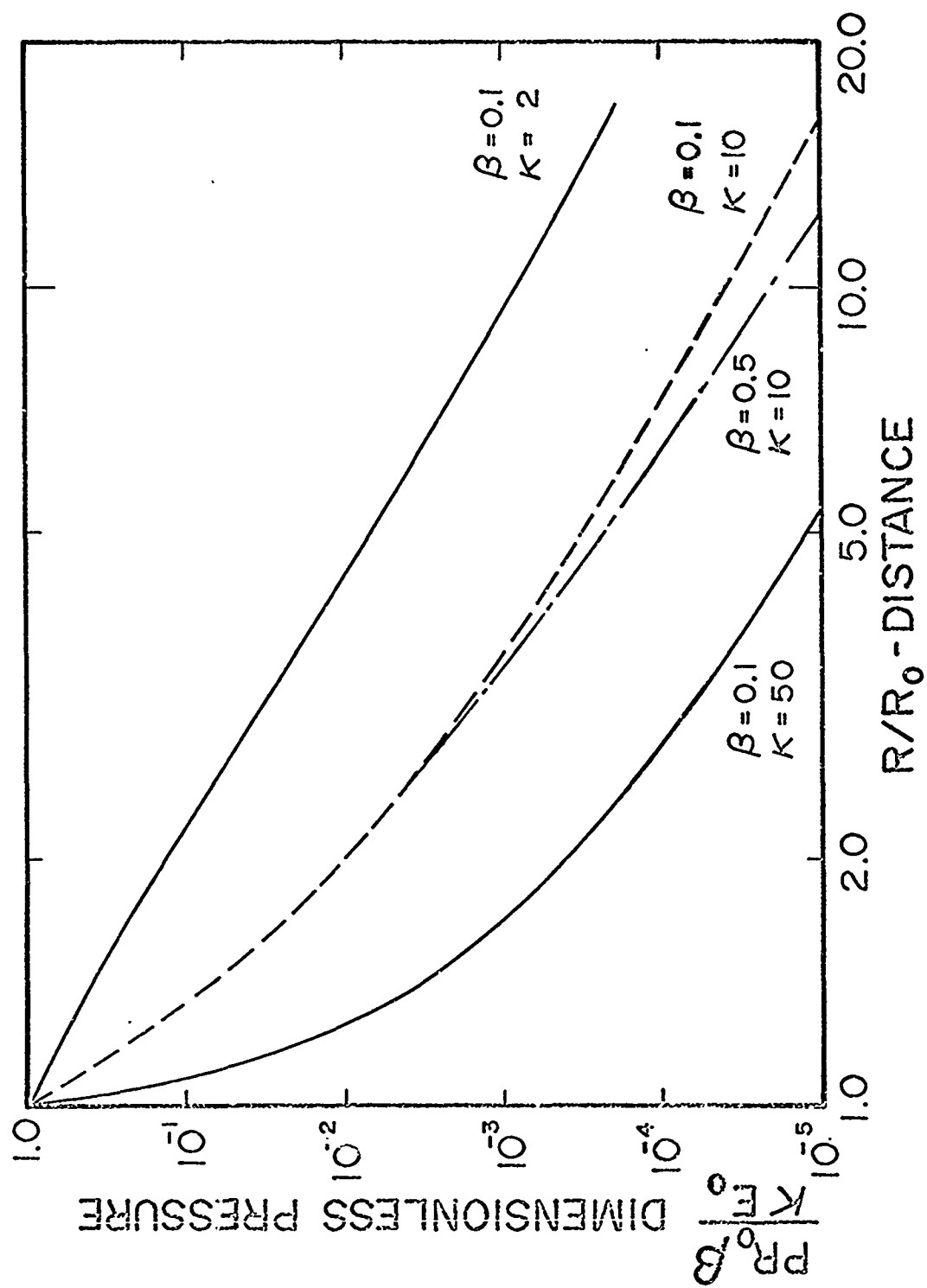
30

Figure 11 Attenuation of Cylindrical Shock Wave in Various Porous Materials --
Shock Generated by Energy Deposition.   Energy Model

31

and

$$W = \frac{P_o R_o^2}{2(\gamma-1)} \left[1 - (R/R_o)^{2(1-\gamma)} \right] \tag{80}$$

In order to satisfy the requirement that the work done on the porous material (Equation 80) be equal to the change in kinetic and internal energies (Equation 74 and 76), we find the pressure must satisfy the integral equation

$$\frac{P_o R_o^2}{2(\gamma-1)} \left[1 - (\frac{R}{R_o})^{2(1-\gamma)} \right] = \frac{\beta P R^2}{2(1-\beta)} \ln \frac{R}{R} + \frac{\beta}{2} \int_{R_o}^{R} P(\xi) \xi d\xi \tag{81}$$

Solutions of this non-singular equation were obtained by numerical integration and are given on Figure 12 for various values of β.

d. A Simple Energy Model

The equality of the internal energy and the kinetic energy at the shock front noted earlier (Equation 62) suggests a simplifying approximation, namely, that the total energy behind the front might be equally divided between the total kinetic energy and the total internal energy.

For the case of an instantaneous deposition of energy, it then follows that

$$\epsilon_o R_o^2 d\phi^2 = 2E_K \qquad \text{for the spherical case}$$

$$\epsilon_o R_o d\theta dz = 2E_K \qquad \text{for the cylindrical case}$$

where E_K is given by Equations 59 and 74, respectively.
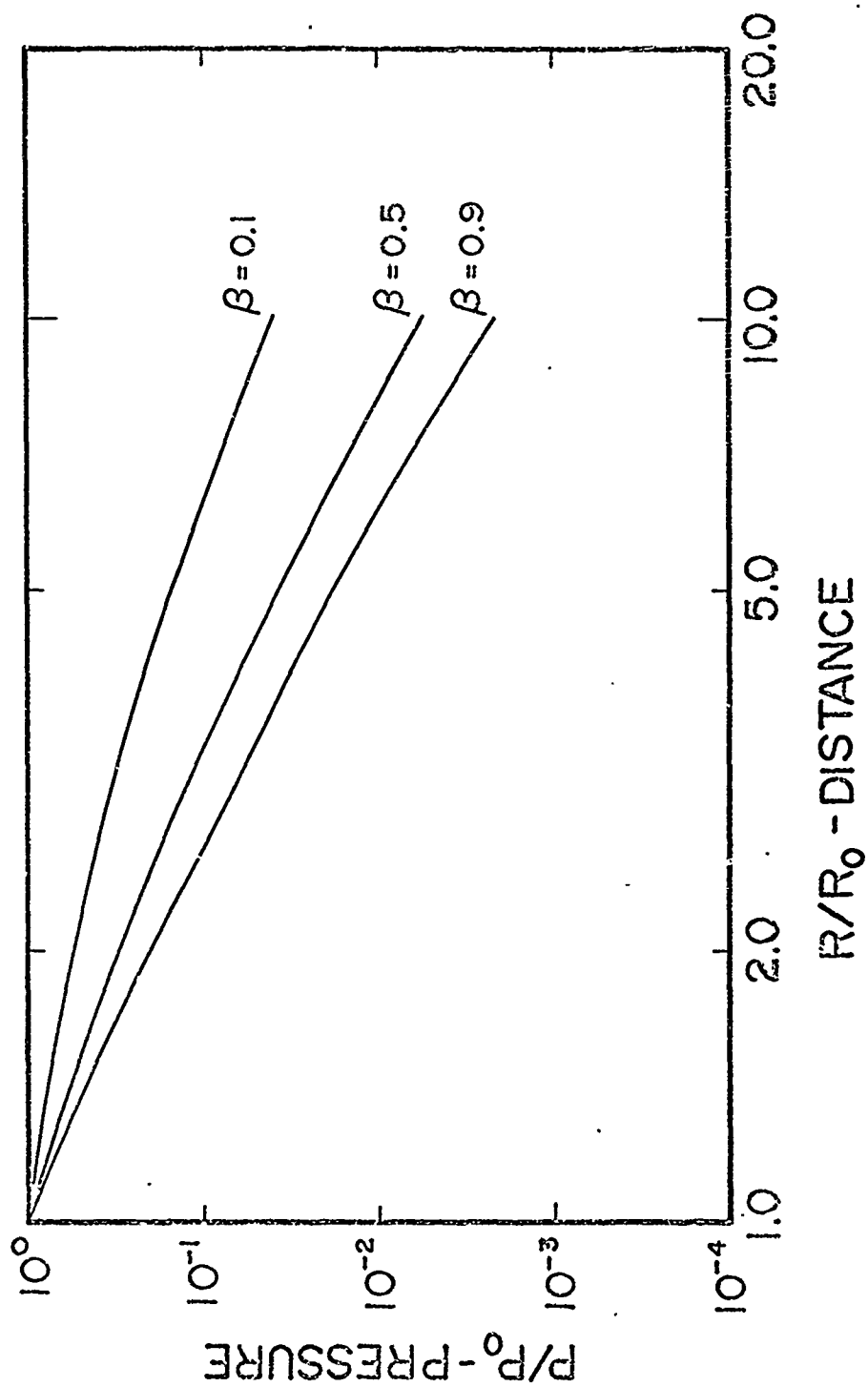
The results are:

For the spherical wave

32

Figure 12 Attenuation of Cylindrical Shock Wave in Various Porous Materials -

Shock Generated by Cavity Expansion. Energy Model with $\gamma = 5/3$

33

$$\frac{P(R)R_0}{\epsilon_0} = \frac{(1-\beta)}{\beta} \frac{1}{(\frac{R}{R_0})^3(\frac{R}{R}-1)} \tag{82}$$

and

$$\frac{P(R)R_0}{\epsilon_0} = \frac{(1-\beta)}{\beta} \frac{1}{(\frac{R}{R_0})^2 \ln(\frac{R}{R})} \tag{83}$$

for the cylindrical wave.

For the cavity expansion models, the simplifying assumption leads to

$$W = 2E_K$$

where the work done by the expansion and the total kinetic energy are given by Equations 70 and 59 for the case of the spherical case, and by Equations 80 and 74 for the cylindrical wave. The results for the spherical wave are

$$\frac{P}{P_0} = \frac{(1-\beta)}{3\beta(\gamma-1)} \frac{\left[1-(R_0/R)^{3(\gamma-1)}\right]}{(\frac{R}{R_0})^3 \left[\frac{R}{R}-1\right]} \tag{84}$$

and for the cylindrical wave

$$\frac{P}{P_0} = \frac{(1-\beta)}{2\beta(\gamma-1)} \frac{[1-(R_0/R)^{2(\gamma-1)}]}{(R/R_0)^2 \ln(R/R)} \tag{85}$$

The pressure distance relationship predicted by Equation 84 is shown for several values of β in Figure 13 and are indicated by $N = 3$. Some results for the cylindrical wave (Equation 85) are also given on Figure 13 for several β, and are denoted by $N = 2$.
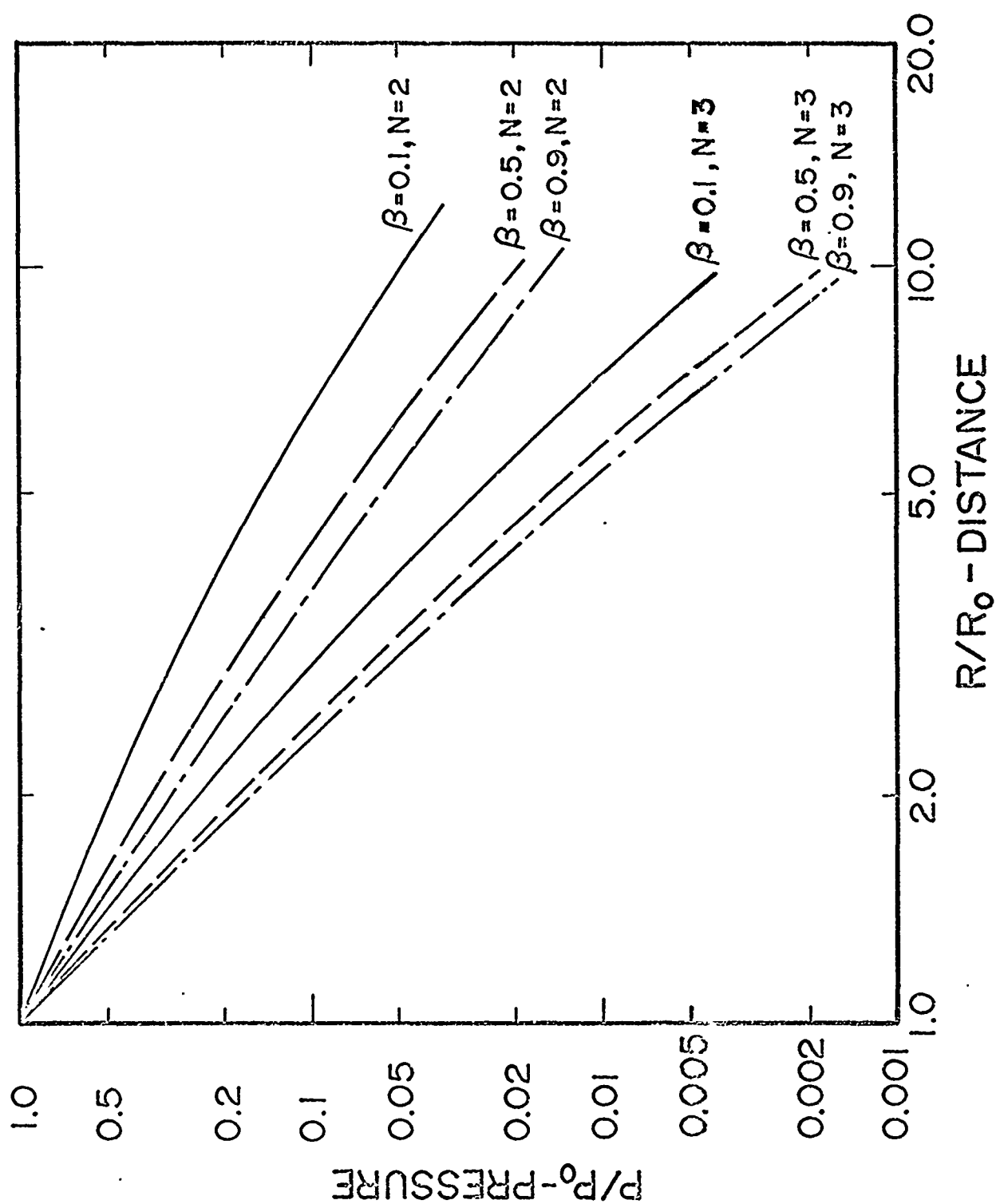
34

Figure 13 Attenuation of Diverging Shock Waves in Porous Materials.

Simplified Model

35

IV. Comparison of Various Models

A comparison of the pressure-distance predictions obtained through the use of several models is given in Fig. 14 for the case of $\beta = .065$ and cylindrical waves.

In each case, a dimensionless pressure is presented as a function of distance. In the three cavity expansion models, (curves B, D and F) the pressure is P/P_o, where P_o is the initial pressure in a gas of $\gamma = 5/3$. For the "snowplow" model, Curve A, the dimensionless pressure is $P\rho_f R_o^2/I_o^2$. For the two energy deposition models, Curves C and E, the dimensionless pressure is PR_o/ϵ_o.
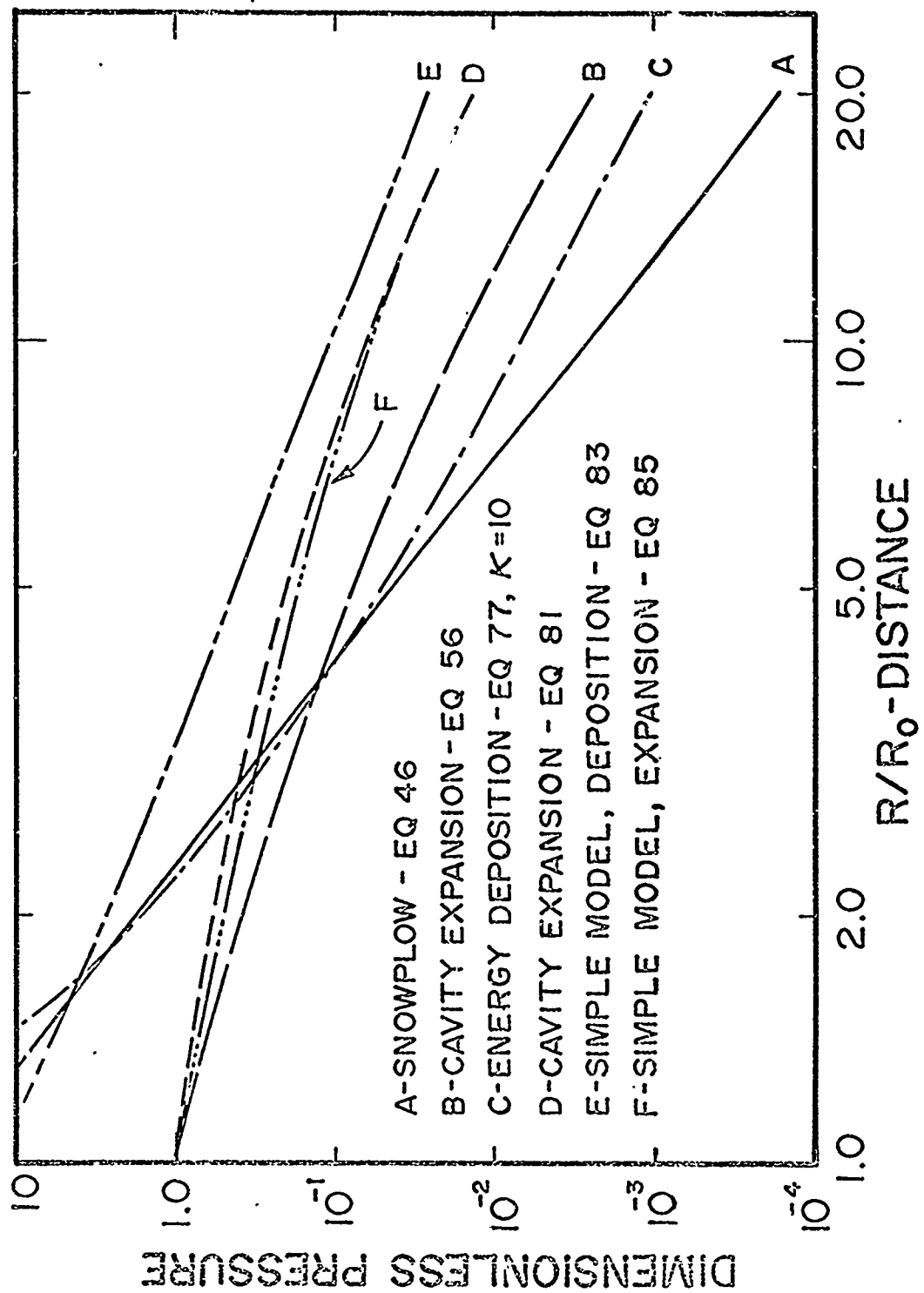
36

Figure 14 Predictions of Various Models for Porous Material of β = .065

V. Summary

Several models for predicting the rate of attenuation of the shock wave generated by an explosion of cylindrical or spherical charges within porous material have been proposed. The porous material is, in all cases, described as an ideal locking solid. Models based on conservation of momentum and on conservation of energy are described. Each model satisfies conservation of mass or conservation of momentum; none satisfy both and therefore all are to be regarded as only approximations.

In the case of spherical waves, it is to be noted that rate of decay can be very high, ranging from the inverse sixth power at large distances for the spherical "snowplow" model down to the third power at large distances for the simplified energy models. The decay rates for cylindrical waves were found to range from an inverse fourth power (in the case of the "snowplow" model) down to the second power for the simplified energy model.

From the pressure distance relationship, the peak particle velocity can be determined as a function of distance by using Equation 16; decay exponents for particle velocities always being one-half those cited above for pressures. Likewise, the shock velocity can be determined as a function of distance by using Equation 8, and can then be integrated (numerically) to give the shock trajectory, if desired. The time required for the shock to propagate to some distance R is

$$t_R = \beta \int_{R_0}^{R} \frac{dR}{V(R)} \tag{86}$$

The particle displacement for a particle originally a distance r from the origin is, at the time the shock has propagated a distance R,

$$U(R, r) = \left[R^3 - (1-\beta)(R^3 - r^3) \right]^{1/3} - r \qquad (87)$$

The use of 87 would seem to predict infinite displacement, at large time, of all points behind the shock. However, it must be noted that the application of all these models must be restricted to times (shock radii) sufficiently small that the shock speed is greater than the speed of an acoustic wave. Combining Equations 16 and 8 yields

$$P(R) = \rho_0 \beta D(R)^2 \qquad (88)$$

Thus all models are invalid for pressures below $\rho_0 \beta C_0^2$, where C_0 is the speed of an acoustic wave in the porous material, and should be considered to be of questionable validity for pressures near this value.

References

1) Herrmann, Walter "Constitutive Equations for Compaction of Porous Materials" Sandia Laboratories Report SC-DC-71 4134, July 1971 presented at the Symposium on Applied Mechanics Aspects of Nuclear Effects in Materials, ASME Winter Annual Meeting, December, 1971.

2) Salvadori, M. G., Skalak, R. and Weidlinger, P. "Spherical Waves in a Plastic Locking Medium," Journal of the Engineering Mechanics Div., ASCE, Vol. 87, No. EM1, February 1961.

3) Gradshteyn and Ryzhik, Table of Integrals, Series and Products, Trans by A. Jeffrey, Academic Press, N. Y., 1965, p 75.

Acknowledgments